ρ_2, T_2, specific density and temperature of the gas inside the closed volume; f, φ, ψ, dimensionless parameters; $m = U_1/V$, outflow rate; $y = \rho_2/\rho_1$; $\Theta = (aF_c/kF) + 1$.

LITERATURE CITED

1. S. Dushman and J. M. Lafferty (editors), Scientific Foundations of Vacuum Technique, Wiley, New York (1962).
2. Yu. Z. Bubnov, M. N. Libenson, M. S. Lur'e, and G. A. Filaretov, Inzh.-Fiz. Zh., 27, No. 3 (1969).
3. I. P. Kalinkin, K. K. Murav'eva, I. B. Yurgel', V. B. Aleskovskii, and I. N. Anikin, Izv. Akad. Nauk SSSR, Ser. Neorg. Mater, 6, No. 9 (1970).

MASS TRANSFER IN CONDENSATION OF VAPOR FROM A FLOW OF FOG-CONTAINING VAPOR – GAS MIXTURE

Ya. M. Vizel', D. I. Lamden, and I. L. Mostinskii

UDC 536.423.4

Results are presented for the experimental settling of fog on the internal wall of a channel from a vapor–air mixture moving along it. Variation of fog concentration was determined by measurement of the intensity of scattered light. Experiment and theory are compared.

The analogy between the processes of heat and mass transfer is valid for condensation of a vapor on a cold surface from a flow of superheated or slightly supersaturated vapor–gas mixture. For a high degree of supersaturation, the intensity of mass transfer is determined not only by diffusion of vapor to the condensation surface but also by the settling of particles of condensed aerosol on it. The latter process is often predominant, and many specialists are engaged in a study of it.

The existing experimental work in this field can be divided into two groups. In the first group are studies of the settling of a fog which is formed by the artificial introduction of condensation nuclei [1, 2]. The rate of aerosol settling was determined either from the deflection of a beam of "developed" nuclei in a transparent vessel [1] or from measurements of the dust concentration introduced into the condenser and of the dust concentration emerging from it [2]. As a rule, the introduction of condensation nuclei makes it possible to distinguish in purer form the settling of an aerosol from the overall process of mass transfer during the flow of a vapor–gas mixture.

In the second group of experimental work are studies of the settling of a fog formed by homogeneous condensation of a vapor in the flow of a vapor–gas mixture. In [3, 4], the total flow rate was measured for a condensate which was formed as the result of simultaneously occurring processes of surface condensation and fog-particle settling. The relative contributions of the two processes were determined by theoretical methods only.

In the present work, a fog which was formed by homogeneous condensation before entrance into the experimental section was used as the nucleus. In this case, we measured and calculated both the total amount of condensate which settled on the wall and the variation of aerosol concentration in the flow along the condenser.

The experimental device (Fig. 1) is in the form of a closed loop through which air is pumped by the centrifugal fan 1. After leaving the fan, the air passes through the straight section 2 and the gas-flow meter 3 (for turbulent flow, this is a normal venturi; for laminar flow, it is an RS-5 rotameter). Then the air is fed into the gas heater 4, into which water vapor from the vapor generator is also fed, and into the chiller 5. The gas heater and chiller are two sequentially installed pipes with an internal diameter of 95 mm in which straight-

Institute of High Temperatures, Academy of Sciences of the USSR, Moscow. Translated from Inzhenerno-Fizicheskii Zhurnal, Vol. 29, No. 6, pp. 1000–1006, December, 1975. Original article submitted July 2, 1974.

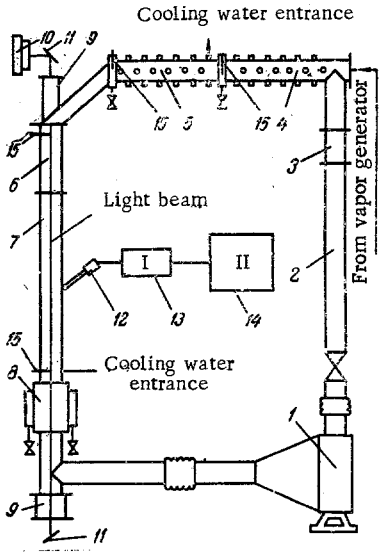

Fig. 1. Diagram of experimental device. I) photomultiplier, and II) digital voltmeter.

through tubing is soldered perpendicularly to the pipe axis. To improve heat transfer, the tubing is alternated in mutually perpendicular planes. In the gas heater, Nichrome heating elements are installed inside the tubing; in the condenser, tap water flows through the tubing.

Following this, the vapor–gas mixture is fed into the thermally-insulated channel 6, 20 × 80 × 500 mm in size, which acts as a thermal and hydrodynamic stabilization section. The experimental section 7 immediately following is in the form of a rectangular channel 20 × 80 × 1210 mm in size. The wide wall is cooled by running water and there are windows of optical glass in the narrow wall. The vertical section of the loop ends in the condensate collector 8 following which the vapor–gas mixture is fed back to the fan. Above the stabilization section and below the experimental section there are the fittings 9 with heated optical-glass inserts for vertical illumination and adjustment of the light beam along the condenser axis.

The temperature of the gas flow is measured at the beginning and end of the chiller and also before entrance into the stabilization section and after leaving the experimental section by means of the thermocouples 15 which are in thin sleeves. The temperature of the walls of the stabilization and experimental sections is measured at 74 points, which makes it possible to follow the lengthwise variation of temperature most thoroughly. The vapor content before entrance into the chiller is determined from the dew point. The temperature is controlled by changing the current to the gas heater and the temperature range over which condensate tracks appear and vanish is no more than 2°C. During an experiment the output of the vapor generator is also measured along with the condensate flow rate beyond the chiller and beyond the experimental section.

The experimental section is illuminated from above downwards by a beam from the helium–neon laser 10 which is directed by the mirror system 11. The light intensity scattered by fog particles at various angles to the flow axis is determined by means of the ebonite collimating sight 12, which is connected to the FÉU-77 photomultiplier 13 by a fiber light-pipe; the signal from the photomultiplier is recorded by the digital voltmeter 14. Movement of the sight along the channel, its setting at various angles, and adjustment with respect to the beam are accomplished by means of a special locater.

The determination of the mean size of aerosol particles was based on the ratio of light intensities scattered at two angles (45° and 135°) using the technique proposed in [5]. The relative variation of aerosol-particle concentration along the beam was determined both from scattering at 45° and from scattering at 135° using the data for mean size. Tabulated values of the Mie function [6] were used in the calculations. It should be noted that while the intensity of light scattered at 45° depends strongly on mean size, the size dependence for light intensity scattered at 135° is extremely weak in the range of sizes we produced (around 0.15 μm). This markedly increases the reliability of the results for the variation of particle concentration along the section.

The experiments were performed over the following ranges of the basic parameters: temperature of vapor–gas mixture at entrance to the stabilization section, 314–350 °K; vapor content at the entrance to the experimental section, 0.18–0.55; wall temperature of experimental section, 278–290°K; temperature of vapor–gas mixture at exit from experimental section, 295–330°K; gas velocity, 0.3–9 m/sec, corresponding to Reynolds numbers Re = 600–16,000. In the experiments, the Prandtl and Schmidt numbers remained practically constant and were identical, $Pr \sim Sc \sim 0.7$–0.8.

As shown by calculations using the method in [7], a vapor–gas mixture in a chiller first rapidly becomes supersaturated and then its supersaturation rapidly falls to almost 1 because of the formation of nuclei and the condensation of vapor on them. Since the zone of homogeneous condensation was very short, the aerosol formed was fairly monodisperse. The particle radius was $\sim 1.5 \cdot 10^{-5}$ cm for laminar modes and $\sim 0.5 \cdot 10^{-5}$ cm for turbulent modes. The numerical concentration of particles at the entrance to the stabilization section was determined with consideration given to the escape of condensate after the chiller.

Two processes were considered separately in the calculation of heat and mass transfer within the experimental section: vapor condensation on the walls because of diffusion and settling of fog particles. The entire condenser was divided lengthwise into 10 computational regions in which all parameters were assumed constant and both processes independent of one another; the gradient of vapor concentration over cross section was determined from the gradient of partial saturation pressure.

The calculation of mass transfer for vapor condensation on the wall was carried out in analogy with heat transfer [8]. For turbulent modes, the flow was stabilized before entrance into the condenser, but stabilization did not occur for laminar modes and the entire condenser was in the region of the thermal and diffusion initial section [9].

A calculation of the behavior of fog particles arriving in the experimental section from the chiller using the method of [7] showed that particles change their initial size insignificantly because of condensation growth and vaporization. Homogeneous condensation also can be neglected here because supersaturation is nowhere more than 1.8.

We used relations in [10] to calculate thermal and diffusion phoresis of fog particles. The evaluations made showed that in our experiments, just as in [2], settling because of thermophoresis was small in comparison with diffusion phoresis (no more than 15%).

For the velocity of transverse motion under the action of diffusion phoresis forces we have [10]

$$V_x = -D\,\frac{m_1}{m_2}\cdot\frac{1}{n_2}\left(1+\frac{1+6C_m\dfrac{\lambda}{R}}{1+2C_m\dfrac{\lambda}{R}}\right)\operatorname{grad} n_1. \tag{1}$$

We consider expressions for the capture coefficient δ of aerosol particles [10] which can be obtained with the help of Eq. (1) for each of the computational regions of the experimental condenser. The capture coefficient is defined as the ratio between the number of particles settling on the wall per unit time and the number of particles arriving in the computational region during that same time.

For laminar flow, the distributions of mass velocity and concentration obey a parabolic law:

$$V_z = \frac{3}{2}\,\bar{V}_z\left(1-\left(\frac{x}{h}\right)^2\right), \tag{2}$$

$$n_1 = n_1^{W} + \left(\frac{3}{2}\,\bar{n}_1 - n_1^{W}\right)\left(1-\left(\frac{x}{h}\right)^2\right). \tag{3}$$

We obtain an expression for the capture coefficient by considering the trajectory of particles obeying the equation

$$\frac{dx}{dV_x} = \frac{dz}{dV_z} \tag{4}$$

(the x axis coincides with the flow velocity and the z axis is perpendicular to it; the flow is assumed two-dimensional):

$$(1-\delta)^2 - \ln(1-\delta) = \frac{4l\,(n_1 - n_1^{W})}{\bar{V}_z h^2}\,D\,\frac{m_1}{m_2}\cdot\frac{1}{n_2}\left(1+\frac{1+6C_m\dfrac{\lambda}{R}}{1+2C_m\dfrac{\lambda}{R}}\right). \tag{5}$$

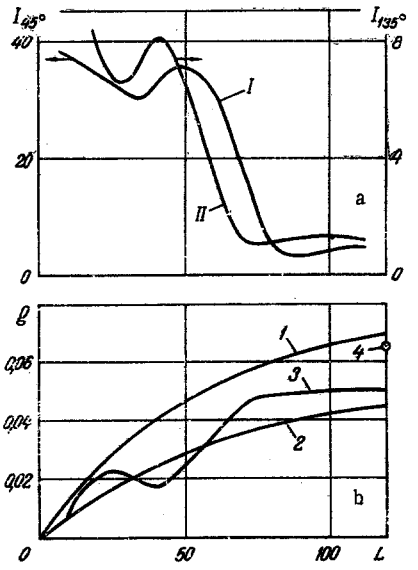

Fig. 2

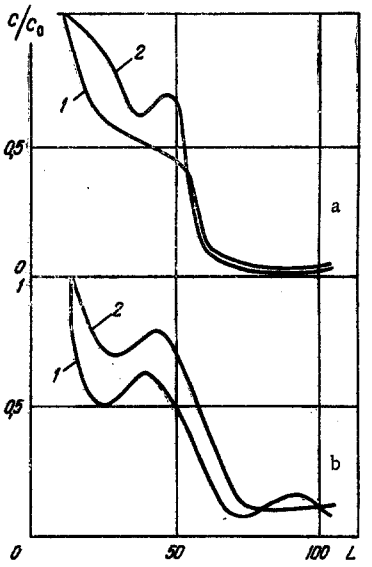

Fig. 3

Fig. 2. Variation of relative intensity of light scattered by fog (a) and of amount of fluid settling (b) along the channel length L, cm (Re = 1800): I) at 45°; II) at 135°; 1) total calculated flow rate of fluid settling on the wall (g/sec); 2) settling of aerosol (calculated); 3) settling of aerosol (calculated from variation of luminosity); 4) total amount of settled fluid (experiment).

Fig. 3. Distribution of numerical (1) and mass (2) concentrations of fog along condenser length L, cm: a) Re = 800; b) Re = 1800.

For turbulent flow, the distributions of mass velocity and concentration obey a 1/7 law in the core of the flow and are linear in the laminar sublayer (two-layer model). The thickness of the laminar sublayer for two-dimensional flow can be determined by using the Blasius formula for frictional stress:

$$\frac{\delta'}{2h} = \frac{59.8}{(2\mathrm{Re}_h)^{0.85}}. \tag{6}$$

In calculating the capture coefficient, one can assume that the concentration in the flow core is constant and that a gradient exists only in the viscous sublayer:

$$\delta = D\,\frac{m_1}{m_2}\cdot\frac{1}{\overline{n_2}}\left(1+\frac{1+6C_m\dfrac{\lambda}{R}}{1+2C_m\dfrac{\lambda}{R}}\right)\frac{(\overline{n_1}-n_1^{W})F_1}{\delta'\overline{V}_z F_2\overline{n}_1}. \tag{7}$$

We compare the results of a mass-transfer calculation with experiment. Luminosity of the fog in a laser beam was observed only for laminar modes. This is undoubtedly explained by the large sizes of fog particles, since in this region the greatest intensity of scattered light is proportional to roughly the sixth power of the radius. The variation in intensity of the light scattered at angles of 45° and 135° along the condenser is shown in Fig. 2. This is a typical example (Re = 1800). All other experiments in the laminar mode gave a qualitatively similar pattern. The same figure shows the variation of the flow rate of the aerosol settling along the experimental section calculated from Eq. (5) and obtained from luminosity measurements. The same figure shows, in addition, the calculated total variation of condensate flow rate along the experimental section (including condensation on the wall) and an experimental point (measured condensate flow rate). It is clear from Fig. 2 that although Eq. (5) gives almost the same final result as experiment, the actual nature of the variation in the flow rate of an aerosol settling along the condenser differs from the calculated variation. The difference lies in the fact that there is a short region in the condenser where almost 90% of the fog settles. The drop in concentration in this region varies with variation of Re; it becomes steeper for smaller Re. One should note that the position of the region of intensified settling in the experimental section remained constant in all experiments with laminar flow irrespective of the dependence on the value of Re. For comparison, Fig. 3 shows the variation of the rela-

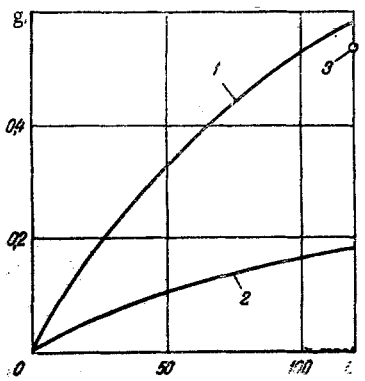

Fig. 4. Variation in amount of fluid settling along the channel length L, cm, in turbulent flow (Re = 12,000): 1) total calculated flow rate of fluid settled on wall, g/sec; 2) settling of aerosol (calculated); 3) experimental point.

tive numerical and mass concentrations of particles along the experimental section for two values of Re: for Re = 800 in Fig. 3a and for Re = 1800 in Fig. 3b. As is clear from these figures, the region of intensified settling of fog is highly elongated when the flow velocity is increased and the relative amount of settling aerosol is decreased.

In the calculation of the capture coefficient, the variation in the radius of fog particles because of vaporization and condensation of moisture on them was taken into account. The radius of fog particles varied along the length of the condenser within limits of ± 30%, which was also verified by calculations based on the ratio of the light intensities scattered at 45° and 135°. It is therefore impossible to explain the existence of a region of intense settling by a variation in particle radius. This problem requires further study.

Figure 4 shows the calculated dependence and an experimental point for a typical experiment in the turbulent mode (Re = 12,000). Rather good agreement between the final result of mass-transfer calculation and experiment is also observed here. A comparison of Figs. 2 and 4 shows that while the main mass of condensate in the laminar mode consists of settled fog particles, deposition of vapor from the flow occurs mainly because of condensation on the walls in turbulent flow.

NOTATION

D, mutual diffusion coefficient for air and water vapor; m_1, m_2, their molecular weights; n_1, n_2, volume concentrations; C_m, diffusion slip coefficient; λ, free path of gas molecules; R, radius of fog particle; δ, capture coefficient; h, half-width of channel; V_z, gas velocity; n_1^w, vapor concentration at wall determined by vapor elasticity at wall temperature; l, length of computational region in experimental section; δ', thickness of laminar sublayer; F_1, F_2, surface condensation area of computational region and cross section of experimental section.

LITERATURE CITED

1. B. V. Deryagin, A. I. Storozhilova, G. I. Shcherbina, and B. A. Obukhov, Dokl. Akad. Nauk SSSR, 201, 651 (1971).
2. A. N. Terebenin and A. P. Bykov, Zh. Fiz. Khim., 45, 1012 (1972).
3. M. A. Styrikovich and I. B. Godik, Izv. Akad. Nauk SSSR, Énerget. Transport, No. 6, 97 (1966).
4. K. M. Aref'ev, V. M. Borishanskii, N. I. Ivashchenko, A. V. Korol'kov, I. I. Paleev, and B. M. Khomchenko, Teplofiz. Vys. Temp., 9, No. 3, 600 (1971).
5. I. Ya. Slonim, Opt. Spektrosk., 8, 98 (1960).
6. K. S. Shifrin and I. L. Zel'manovich, Tables of Light Scattering [in Russian], Vol. 2, Gidrometeoizdat (1967).
7. A. G. Amelin, Theoretical Fundamentals of Fog Formation by Vapor Condensation [in Russian], Khimiya (1972).
8. M. A. Styrikovich, I. L. Mostinskii, and Ya. M. Vizel', Teplofiz. Vys. Temp., 6, 707 (1968).
9. B. S. Petukhov, Heat Transfer and Resistance in Laminar Fluid Flow in Pipes [in Russian], Énergiya (1967).
10. Yu. I. Yalamov and E. R. Shchukin, Inzh.-Fiz. Zh., 24, No. 2 (1973).